



SCIENCE AND TECHNOLOGY ORGANIZATION
CENTRE FOR MARITIME RESEARCH AND EXPERIMENTATION



Reprint Series

CMRE-PR-2014-005

Range estimation of cetaceans with compact volumetric arrays

Walter M.X. Zimmer

January 2014

Originally published in:

Journal of the Acoustical Society of America, Vol. 134, No. 3, 2013, pp. 2610-2618

About CMRE

The Centre for Maritime Research and Experimentation (CMRE) is a world-class NATO scientific research and experimentation facility located in La Spezia, Italy.

The CMRE was established by the North Atlantic Council on 1 July 2012 as part of the NATO Science & Technology Organization. The CMRE and its predecessors have served NATO for over 50 years as the SACLANT Anti-Submarine Warfare Centre, SACLANT Undersea Research Centre, NATO Undersea Research Centre (NURC) and now as part of the Science & Technology Organization.

CMRE conducts state-of-the-art scientific research and experimentation ranging from concept development to prototype demonstration in an operational environment and has produced leaders in ocean science, modelling and simulation, acoustics and other disciplines, as well as producing critical results and understanding that have been built into the operational concepts of NATO and the nations.

CMRE conducts hands-on scientific and engineering research for the direct benefit of its NATO Customers. It operates two research vessels that enable science and technology solutions to be explored and exploited at sea. The largest of these vessels, the NRV Alliance, is a global class vessel that is acoustically extremely quiet.

CMRE is a leading example of enabling nations to work more effectively and efficiently together by prioritizing national needs, focusing on research and technology challenges, both in and out of the maritime environment, through the collective Power of its world-class scientists, engineers, and specialized laboratories in collaboration with the many partners in and out of the scientific domain.



Copyright © Acoustical Society of America, 2013. NATO member nations have unlimited rights to use, modify, reproduce, release, perform, display or disclose these materials, and to authorize others to do so for government purposes. Any reproductions marked with this legend must also reproduce these markings. All other rights and uses except those permitted by copyright law are reserved by the copyright owner.

NOTE: The CMRE Reprint series reprints papers and articles published by CMRE authors in the open literature as an effort to widely disseminate CMRE products. Users are encouraged to cite the original article where possible.

Range estimation of cetaceans with compact volumetric arrays

Walter M. X. Zimmer^{a)}

Centre for Maritime Research and Experimentation, NATO, Viale le San Bartolomeo 400,
19138 La Spezia, Italy

(Received 27 August 2012; revised 12 April 2013; accepted 24 July 2013)

Passive acoustic monitoring is the method of choice to detect whales and dolphins that are acoustically active and to monitor their underwater behavior. The NATO Science and Technology Organization Centre for Maritime Research and Experimentation has recently implemented a compact passive acoustic monitor (CPAM), consisting of three arrays of two hydrophones each that are combined in a fixed three-dimensional arrangement and that may be towed at depths of more than 100 m. With its volumetric configuration, the CPAM is capable of estimating the three-dimensional direction vector of arriving sounds and under certain conditions on relative geometry between the whale and hydrophone array, the CPAM may also estimate the range to echolocating animals. Basic ranging methods assume constant sound speed and apply straightforward geometry to obtain depth and distance to the sound source. Alternatively, ray-tracing based methods may be employed to integrate the information provided by real sound speed profiles. Both ranging methods combine measurements of sound arrival angles and surface reflection delays and are easily implemented in real-time applications, whereby one could promote the ray-tracing approach as the preferred method because it may integrate real sound speed profiles. © 2013 Acoustical Society of America. [<http://dx.doi.org/10.1121/1.4817892>]

I. INTRODUCTION

Passive acoustic monitoring (PAM) is increasingly used by the scientific community to study, survey, and census marine mammals, especially cetaceans, some of which are easier to hear than to see. PAM is also requested to support efforts to mitigate potential negative effects of human activities such as ship traffic, military and civilian sonar, and offshore exploration on cetaceans, particularly those species that were found to react significantly to anthropogenic sound (see, e.g., [Simmonds and Lopez-Jurado, 1991](#); [Frantzis, 1998](#), for sonar related beaked whale strandings).

PAM is a good technique for surveying and studying cetaceans, not only because these animals frequently use sound for their day-to-day activities, but also because acoustics is so far the only tool that allows the study of submerged animals and that are therefore not visible to human observers. At the same time, PAM does not interfere with the animal's behavior if properly implemented. Overall, PAM is expected to improve the overall capability to monitor the temporal and spatial behavior of cetaceans and therefore their habitat usage ([Barlow and Gisiner, 2006](#)).

Beaked whales (family Ziphiidae) are deep divers and for that reason rarely visible at the surface ([Barlow, 1999](#)) while acoustically active when engaged in deep foraging dives that may exceed 1000 m ([Tyack et al., 2006](#)). Because of their apparent sensitivity to sonar type sound ([Cox et al., 2006](#); [Tyack et al., 2011](#)), beaked whales in general and Cuvier's beaked whales (*Ziphius cavirostris*, in short Zc) in particular, are of interest for the Active Sonar Risk Mitigation (ASRM) program at the NATO Centre for Maritime Research and Experimentation (CMRE, formerly

NURC and SACLANCEN) and consequently, one of the program objects is the development and assessment of passive acoustic detection and ranging tools of Cuvier's beaked whales. Localization of beaked whales is not only an important aspect if one is interested in mitigating adverse effects of sound on cetaceans, but also if one wants simply to estimate their abundance ([Buckland et al., 2001](#)).

The performance of passive acoustic detection of Cuvier's beaked whales was analyzed by [Zimmer et al. \(2008\)](#) and was found to be range limited due to the increased attenuation of the ultra-sonic sounds (9.5 dB/km at 40 kHz) of the whales and the dependency on their detailed behavior during foraging. In good environmental conditions, acoustic activities of Cuvier's beaked whales may be detected with near certainty up to about 1 km, but detection ranges beyond 5 km are very unlikely and require extremely low ambient noise or special conditions in sound propagation. Complicating factors are the variability of the temporal and spectral signal characteristics that are mostly due to the varying orientation of the clicking animal and to voluntary variation in sound source levels ([Zimmer et al., 2008](#)).

Estimating the actual range to clicking animals is a pre-requisite for determining the detection function that is fundamental for most ecological studies. There is a variety of passive acoustic-based methods to obtain the range to an animal, depending on the quality and quantity of measurements. Multi-hydrophone ranging may use spatially distributed hydrophones and estimates 2D and/or 3D location of the sound source ([Watkins and Schevill, 1977](#); [Spiesberger and Fristrup, 1990](#); [Wahlberg et al., 2001](#); [Ward et al., 2008](#); [Zimmer, 2011](#), p. 198ff). Towed arrays with closely spaced hydrophones may be used to obtain source direction by beamforming allowing limited ranging by sequential triangulation (e.g., [Zimmer et al., 2003](#)).

^{a)}Electronic mail: zimmer@cmre.nato.int

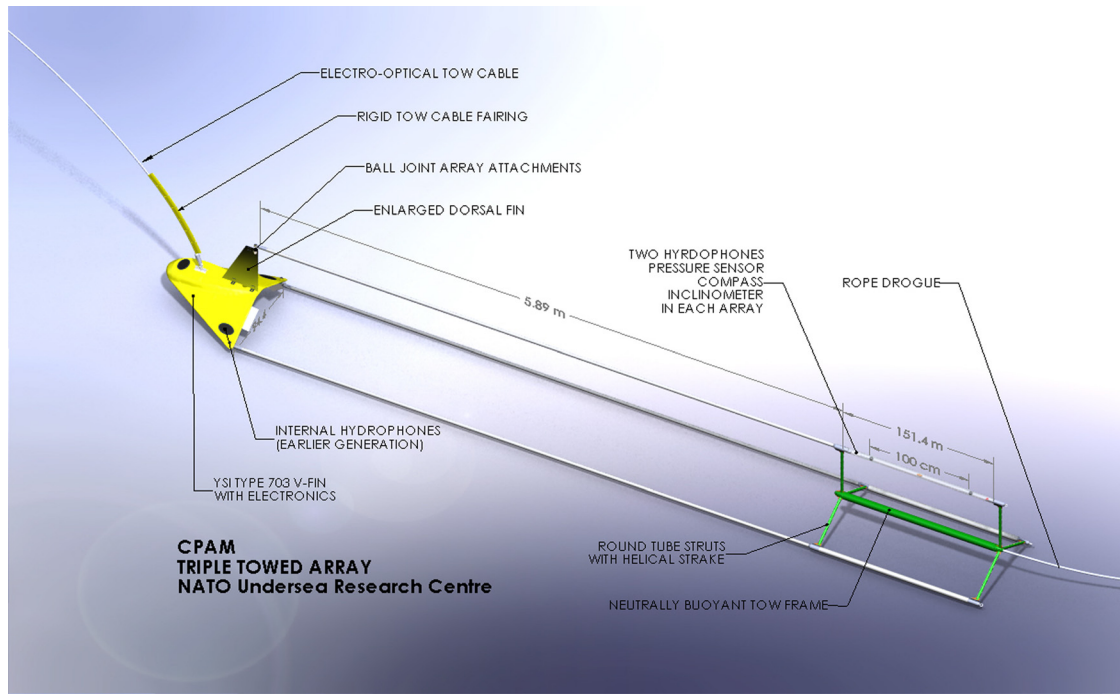


FIG. 1. (Color online) CPAM triple towed array assembly.

While the estimation algorithms are trivial, the hardware and operational costs may be substantial. Multi-path ranging, on the other hand, uses only a single hydrophone and exploits the complex multi-path structure of the arriving sound to estimate range and depth of the acoustically active animal (Thode, 2004; Nosal and Frazer, 2006; Zimmer, 2011, p. 205ff). The advantages of reduced hardware requirements are countered by the need of good knowledge of the bathymetry between hydrophone and sound source. In addition, any acoustic ranging method needs knowledge of the sound speed between animal and receivers. A zeroth order approximation assumes a constant sound speed (isovelocity), somewhere around 1500 m/s and with this assumption, all ranging calculus reduces to geometry. However, such isovelocity conditions rarely exist in real oceans and more complicated ranging procedures reflecting the anisotropy in sound speed should be considered for range estimation. Frequently, ray-trace acoustic propagation models are used to integrate varying sound speeds into the ranging process (e.g., Thode, 2004; Nosal and Frazer, 2006; Tiemann *et al.*, 2006). This approach typically determines the received sound time series as a function of varying sound locations and determines the best sound locations by the best fit between modeled and measured data, i.e., where the measurement-model mismatch becomes minimal.

Traditional cetacean research uses line arrays that have one significant limitation, as the obtained directions are not unique with regard to rotational symmetry of line arrays. To overcome this drawback, one must distribute the hydrophones in two or three dimensions resulting in different possibilities to implement an array. Watkins and Schevill (1977) deployed from a drifting boat a three-dimensional array with a hydrophone separation of 30 m to track sperm whales. Clark (1980) obtained the direction to southern right whales

using a compact 3-element two-dimensional array. Thode (2004) used a towed tandem array consisting of two sub-arrays separated by 200 m towed in parallel with a second standard bio-acoustic array to obtain three-dimensional tracks of sperm whales. Hirotsu *et al.* (2010) used two four-hydrophone array systems to estimate the distance of sperm whales by triangulations using the directions of the two compact arrays. Wiggins *et al.* (2012) tracked beaked whales with a four hydrophone small-aperture array (configured as a tetrahedron with approximately 0.5-m sensor spacing) that was coupled to an autonomous acoustic recorder to obtain swimming and diving behavioral information for free-ranging animals using a single instrument. Compact volumetric arrays are also becoming valuable tools for bio-acoustic analysis of cetacean sounds. For example, small four-hydrophone arrays were used to measure echolocation signals by cetaceans, e.g., killer whales (Au *et al.*, 2004), or from free-ranging white-beaked dolphins (Rasmussen *et al.*, 2002).

So far, compact volumetric arrays were used in mainly stationary applications. Here an acoustic ranging technique is presented that exploits the direction finding capability of a small volumetric towed array, nominated compact passive acoustic monitor (CPAM). This system was developed in recent years at the CMRE and uses, in addition to the three-dimensional source direction, the time delay of surface reflections to determine range and depth of acoustic sources. Ranging is implemented as straight forward geometric localization but also by means of ray-tracing to address the refraction of the sound rays in environments where the sound speed varies as function of depth. The performances of both ranging methods are compared and the differences discussed. Both methods are applied to real data that were collected by the CMRE during the 2011 Sirena11 cetacean survey in the Ligurian Sea.

II. THEORY

The present ranging technique was developed to exploit all the capabilities of the CMRE's compact passive acoustic monitoring (CPAM) system (Fig. 1). The CPAM features 3 towed arrays in volumetric configuration but with fixed geometry. Each array carries 2 hydrophones that are separated by 1 m and a tilt compensated digital compass. The three arrays are separated by 96 cm. The hydrophones are sampled at 192 kHz, and the digital compass that includes a pressure sensor of the top array was used to determine the orientation and depth of the CPAM arrays. The digital compass was sampled at 5 Hz providing pitch, roll, and heading with a nominal accuracy of 1° . The depth sensor was a Kulite 25 BARA pressure sensor and was also sampled at 5 Hz, but with 24 bit resolution.

Ranging with a compact volumetric array consists of two steps: First, the direction of an acoustic source is determined; second, the range is estimated by means of the delay of the surface reflection.

Figure 2 presents an example of a Z_c click (Zimmer *et al.*, 2005) as received with the CPAM. Both, the direct arrival (left side of Fig. 2) and the surface reflected arrival (right side of Fig. 2) are shown. The top two hydrophones are located in the top array and it is therefore clear that the direct arrival at the CPAM arrives from below (click on hydrophone 5 trails the ones on hydrophones 1 and 3) and the surface reflection arrives from above (click on hydrophone 5 is before the ones on hydrophones 1 and 3). The surface reflected click is significantly longer than the direct arriving click, indicating an extended interaction with the surface as the result of sea surface roughness and multiple reflection points.

As the present work deals with localization of cetaceans, the detection process is only briefly described. The hydrophone data were first matched filtered with a synthetic Z_c replica and passed through a Page-test detector (Page, 1954; Zimmer, 2011, p. 133ff). Any detector that provides start time of an acoustic signal would be appropriate (e.g., Zimmer, 2011, p. 119ff). For this work, an acoustically

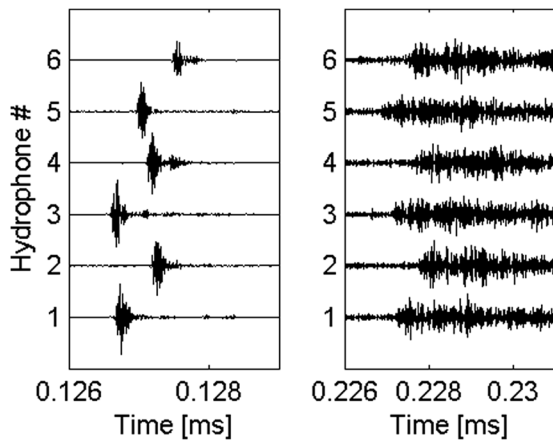


FIG. 2. Multi-channel arrival of a Cuvier's beaked whale click as recorded by the CPAM. (left) Direct arrival, (right) surface reflected signal. Hydrophones 1 and 2 are from array one (starboard), 3 and 4 from second array (port-side), 5 and 6 from top array. Hydrophones with odd numbers are in front of the hydrophones with even numbers.

relevant event was declared if for a given period at least one detection occurred per hydrophone channel. This period was chosen to cover twice the maximal delay that could be measured across the array to allow arbitrary arrival angles. This procedure resulted in a significant reduction of false alarms, as false detections in individual hydrophones were ignored.

For the presented ranging methods, two types of delay measurements were needed: First, an intra-array delay for the same acoustic event to determine the angle of arrival, and second, an inter-detection delay between sound arrivals of a direct and surface-reflected path to estimate the range of the sound source.

A. Direction finding

The direction of the sound source is here estimated by determining for the same signal the relative delays between the different hydrophones and by considering the well known relation between measured delays and the direction vector of the sound source (e.g., Zimmer, 2011, p. 212f).

The sound direction \hat{s} is estimated by (Zimmer, 2011, p. 215)

$$\hat{s} = c\mathbf{M}(\mathbf{D}_0\mathbf{D}_0^T)^{-1}\mathbf{D}_0(\delta\tau), \quad (1)$$

where

$$\hat{s} = \begin{pmatrix} s_x \\ s_y \\ s_z \end{pmatrix}, \quad \delta\tau = \begin{pmatrix} \delta\tau_1 \\ \delta\tau_2 \\ \vdots \\ \delta\tau_N \end{pmatrix}, \quad \mathbf{D}_0^T = \begin{pmatrix} d_{1x} & d_{1y} & d_{1z} \\ d_{2x} & d_{2y} & d_{2z} \\ \vdots & \vdots & \vdots \\ d_{Nx} & d_{Ny} & d_{Nz} \end{pmatrix} \quad (2)$$

and \mathbf{M} is the three-dimensional rotation matrix of the volumetric array; c is the sound speed between the hydrophones.

The arrival angles azimuth φ and elevation ϑ of the sound are finally estimated by solving

$$\tan \varphi = \frac{-s_y}{s_x} \quad (3)$$

and

$$\sin \vartheta = s_z \quad (4)$$

or alternatively

$$\tan \vartheta = \frac{s_z}{\sqrt{s_x^2 + s_y^2}}. \quad (5)$$

As the azimuth angles may vary from -180° to 180° , the solutions of Eq. (3) require the usual care for $s_x < 0$, i.e., by using the four-quadrant inverse tangent. The minus sign in Eq. (3) is simply due to the convention that positive azimuth is measured toward starboard. Equation (5) is preferred to Eq. (4), because, similar to Eq. (3), also Eq. (5) is insensitive to a common factor (e.g., uncertain sound speed at the array). As the elevation angle ϑ is restricted to $\pm 90^\circ$, an ordinary inverse tangent is sufficient for solving Eq. (5).

The minimal number of hydrophones to form a volumetric array is 4 which allows to form $N = 6$ different hydrophone

pairs. While direction finding could be done with only 3 hydrophone pairs, the use of all 6 different combinations should improve the performance, as the impact of measurement errors is reduced. This is reflected by the least-mean-square notation in Eq. (1). Also, using all possible hydrophone pairs puts the reference location of the array automatically in the center of the array eliminating the need for a selection of a reference hydrophone.

A volumetric array with 6 hydrophones allows the formation of $N=15$ different pairs of hydrophones. The CPAM, as used in 2011 and from which Fig. 2 results, featured 6 hydrophones in 3 line arrays and therefore Eq. (1) will later be used with $N=15$ different hydrophone pairs.

B. Geometric localization

Once the arrival angles of the sound are estimated, it may under certain conditions be possible to estimate the location of the sound source. For this to succeed one needs further information. Using an underwater towed array, this can be provided by the surface reflection of the arriving sound. Figure 3 illustrates the concept. Sound is emitted at location W and received at hydrophone H, whereby the sound follows two paths, the short direct path W-H and the longer path W-A-H. For deep diving whales the arrival angle of the direct path is usually negative ($\vartheta_0 < 0$), i.e., whale below the hydrophone, but all surface reflections arrive at the hydrophone from above ($\vartheta_S > 0$). It should be intuitive from Fig. 3 that ϑ_S is always greater than the magnitude of ϑ_0 , that is $\vartheta_S > |\vartheta_0|$.

Assuming a constant sound speed c , one obtains an estimate of animal depth d and range R_0 by the following matrix equation (Zimmer, 2011, p. 209)

$$\begin{pmatrix} d \\ R_0 \end{pmatrix} = \begin{bmatrix} 1 & -\sin\vartheta_0 \\ 4h & -2(c\tau_S)^2 \end{bmatrix}^{-1} \begin{bmatrix} h \\ (c\tau_S)^2 \end{bmatrix}, \quad (6)$$

where ϑ_0 is the elevation angle of the direct sound arrival, h is the hydrophone depth ($h < 0$), and τ_S is the delay between the direct and surface reflected arrival of the same signal.

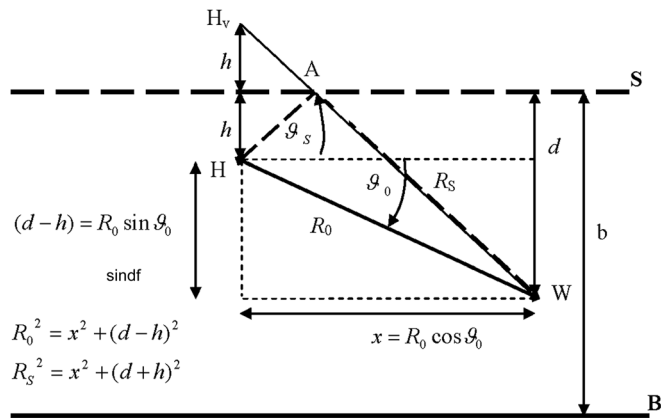


FIG. 3. Schematic for range and depth estimation in case of constant sound speed. **S** indicates the surface, and **B** denotes the bottom. h is the hydrophone depth, d is the whale depth. W is the source and H is the hydrophone location, while H_v is the virtual hydrophone location resulting in a path length H_v -W that is equal to the surface reflected path H-A-W. ϑ_0 is the elevation angle of the direct path (here negative) and ϑ_S is the elevation angle of the surface reflected path as seen on the hydrophone location H.

As with all matrix inversions, a solution does not exist if the matrix is singular, that is, if

$$4h \sin \vartheta_0 = 2(c\tau_S), \quad (7)$$

which would correspond to an infinite range and depth estimate.

The presence of the matrix singularity constrains the allowed surface reflection delays to

$$2h \sin \vartheta_0 < (c\tau_S) < -2h \sin \vartheta_S \leq -2h, \quad (8)$$

whereby the equal sign of the last constraint holds for sounds that are generated just at or directly below the hydrophone, i.e., when $(d-h) = R_0$, or $\vartheta_0 = -\vartheta_S = -90^\circ$.

C. Ray-trace ranging

Geometric ranging [Eq. (6)] can only be applied if the sound speed is constant throughout the water column. In all other cases, where the sound speed varies as a function of depth, Eq. (6) will result in erroneous range and depth estimates of the sound source. In such cases it is better to estimate the location of the sound source by means of ray tracing.

Ray tracing is based on the observation that rays bend as a function of the sound speed gradient. Assuming a horizontally layered ocean and linear variation of the sound speed within each layer, one formulates

$$c(z) = c(z_i) + g_i(z - z_i), \quad (9)$$

for $z_i \leq z < z_{i+1}$ and constant sound-speed gradient g_i .

To implement ray tracing, one first uses Snell's law on refraction to define a constant ray parameter ζ by

$$\zeta = \frac{\cos \vartheta(z)}{c(z)} = \frac{\cos \vartheta(h)}{c(h)} = \text{const}, \quad (10)$$

where $\vartheta(h)$ is the elevation angle of the ray at hydrophone depth and $c(h)$ is the associated sound speed.

The propagation of rays in a piecewise linear sound speed profile is straight forward and may, for example, be found in Jensen *et al.* (2011, p. 208ff). For a ray traveling from depth z_i to z_{i+1} the horizontal distance is estimated by

$$\begin{aligned} x_{i+1} &= x_i + \int_{z_i}^{z_{i+1}} \frac{\cos \vartheta(z)}{\sin \vartheta(z)} dz \\ &= -\frac{1}{\zeta g_i} [\sin \vartheta(z_{i+1}) - \sin \vartheta(z_i)] \end{aligned} \quad (11)$$

and the travel time becomes

$$\begin{aligned} t_{i+1} &= t_i + \int_{z_i}^{z_{i+1}} \frac{dz}{c(z) \sin \vartheta(z)} \\ &= -\frac{1}{g_i} \ln \left[\frac{1 + \sin \vartheta(z_i) \cos \vartheta(z_{i+1})}{\cos \vartheta(z_i) (1 + \sin \vartheta(z_{i+1}))} \right]. \end{aligned} \quad (12)$$

The integration over all layers may then be carried out by summing the integrals of the individual layers

$$X_n(\zeta) = \sum_{i=0}^{n-1} \text{Re}(x_{i+1} - x_i) \quad (13)$$

$$T_n(\zeta) = \sum_{i=0}^{n-1} \text{Re}(t_{i+1} - t_i). \quad (14)$$

By convention, the sums run from the surface to the n th layer at depth z_n and are dependent on the ray parameter ζ , which is defined using the sound speed and the arrival angle at the hydrophone depth. As the arrival angle is used within a cosine function, the ray parameter is insensitive to the sign of the arrival angle, that is, there is no difference for downward or upward rays. This simplifies ray-tracing and makes the presented approach computational efficient.

Equations (13) and (14) are considering only the real part of the integrals to address cases, where the ray does not reach the depth z_{i+1} because it turned earlier into the opposite direction. In the following, it is implicitly assumed that rays that connect hydrophones and whales are independent of the direction of sound, that is, receiver and transmitter may always be exchanged, that is, it is legitimate to assume that the acoustic rays start at the hydrophone and arrive at the whale, while the sound in reality travels from the whale to the hydrophone.

As all rays in Eqs. (13) and (14) are assumed to originate at the surface; one obtains direct or surface reflected rays that initiate at the hydrophone by subtracting or adding the surface-to-hydrophone part of the rays. Let $X_n(\zeta_D; h)$ denote the horizontal distance traveled by the direct ray from the hydrophone depth h to layer n and $X_n(\zeta_S; h)$ be the horizontal distance traveled by the surface reflected ray from hydrophone depth h over the surface to layer n

$$X_n(\zeta_D; h) = X_n(\zeta_D) - X_h(\zeta_D) \quad (15)$$

$$X_n(\zeta_S; h) = X_n(\zeta_S) + X_h(\zeta_S) \quad (16)$$

and let $T_n(\zeta_D; h)$ and $T_n(\zeta_S; h)$ be the corresponding travel time estimates

$$T_n(\zeta_D; h) = T_n(\zeta_D) - T_h(\zeta_D) \quad (17)$$

$$T_n(\zeta_S; h) = T_n(\zeta_S) + T_h(\zeta_S), \quad (18)$$

where the subscript h indicate rays from the surface to the depth of the hydrophone, then Eqs. (15)–(18) describe the rays that originate at the hydrophone.

Varying now the ray parameter ζ_S of the surface reflected ray one finds a depth $z_m(\zeta_S)$ where both rays intersect, that is, where the horizontal distances of the direct ray the surface reflected rays become equal

$$X_m(\zeta_S; h) = X_m(\zeta_D; h). \quad (19)$$

The resulting surface delay is then the time difference between the two rays at the depth of intersection

$$\Delta t_m(\zeta_S) = T_m(\zeta_S; h) - T_m(\zeta_D; h). \quad (20)$$

This procedure results for given hydrophone depth h and ray parameter ζ_D of the direct path in a one-dimensional array that associates for each whale depth $z_m(\zeta_S)$ a time delay for the surface reflection $\Delta t_m(\zeta_S)$. Given a measured time delay τ_S one may then obtain the whale depth by linear interpolation. The horizontal distance is then obtained by virtue of Eq. (19) where the whale depth $z_m(\zeta_S)$ is related to the whale distance $X_m(\zeta_D; h)$. This results in another linear interpolation where one obtains the whale distance as a function of whale depth.

III. EXAMPLE

The following example is presented to demonstrate in more detail the different steps the ray-trace ranging method and to support the performance discussion. The example is based on the sound speed profile measured during Sirena11 and on the measured arrival angle and surface reflection delay that describe the Zc click of Fig. 2. In particular, a measured arrival angle of -35.5° and a hydrophone depth of 123.7 m are assumed.

All surface reflected rays (gray thin lines in Fig. 4) are plotted in steps of 10° for angles that exceed in magnitude the arrival angle of the direct sound path (black line in Fig. 4). The black circles indicate the location (depth and distance) where the direct ray intersects the surface reflected ray paths, that is, where a sound source could be located [i.e., Eq. (19)]. The ensemble of these crossing points provides now a functional relationship between the distance and depth of sound sources. This functional relationship is augmented by the corresponding time delays between the surface reflected and direct ray paths [Eq. (20)].

Figure 5 shows, on the left the sound speed profile and on the right the functional relationship between all possible sound source locations (dashed gray) and the associated time delays (thin black). Both distance and time delay are plotted as functions of depth suggesting the following procedure for ray-trace ranging: Given a measured time delay, here $\tau_S = 0.1004$ s, one obtains first a depth of 1235 m from time-delay curve (solid line) and subsequently one finds a distance

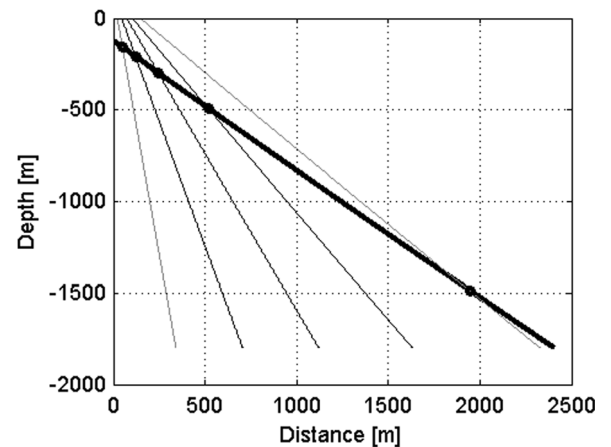


FIG. 4. Selected ray traces where the sound source is below the hydrophone. The thick line is the direct path, the thin lines are the surface reflected paths varying from 40° to 80° (from right to left). The dots mark the crossings direct path and surface reflected paths.

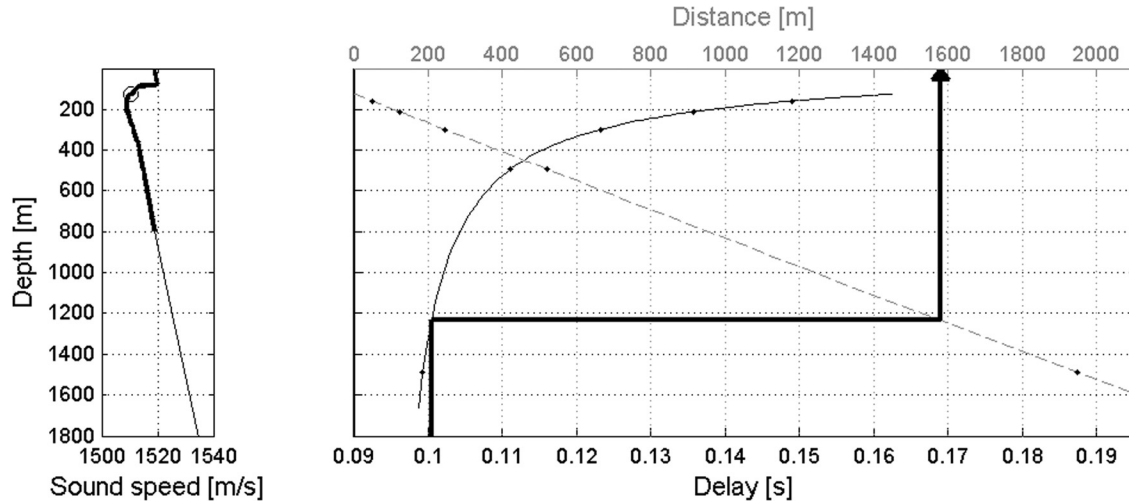


FIG. 5. Visualization of the ray-race ranging for measured time delay of surface reflection ($\tau_S = 0.1004$ s). The sound speed profile is shown on the left side where the measured part is emphasized in black and the extrapolated part is shown in gray. The time-delay to depth functionality is shown on the right side as a solid-dotted line (increasing to the right) and the depth to distance function is given as a dashed-dotted line (linearly decreasing to the right). The dots in both curves correspond to the crossings (dots) in Fig. 4. The thick black line in the right panel describes the ranging process and is described in more detail in the text.

of 1580 m from the distance curve (dashed line). In summary, with the measured sound speed profile, an arrival angle of -35.5° of the direct path, a hydrophone depth of -123.7 m and a surface reflection delay of $\tau_S = 0.1004$ s, the animal is estimated to be at a depth of 1235 m and a horizontal distance 1580 m.

IV. LOCALIZATION OF A SEQUENCE OF ZC CLICKS

In the following, both the geometric and the ray-tracing ranging method will be applied to a sequence of Z_c clicks recorded during Sirena11 and some critical issues that may arise during this type of localization will be discussed. This click sequence is contained in 7.5 s worth of data recorded on 8 December 2012 around 21:00. About 30 detections occurred, 16 of which had negative elevation angles, but only 14 detections formed a confined cluster and were kept for further processing. Figure 6 shows the elevation-azimuth plot of all detections where the 14 detections of interest are marked in solid black. The cluster of gray dots above the black dots is mainly generated by the surface reflections,

whereas its variation is due to uncertainties in the angle estimations.

After defining the direct arrivals of interest, all trailing detections with positive elevation angles were considered as potential surface reflections. Figure 7 shows these potential time delays as a function of click times. One may note from Fig. 7 that 14 potential surface reflections fall inside the allowed time span as given by Eq. (8) (i.e., 94.7 to 164 ms) and that all these 14 detections cluster around 100.69 ms, that is, they can be considered to be valid surface reflections and therefore marked by circles. From Fig. 7, one may also note that the measured travel time delays are close to the lower side of the allowed time span, indicating that one should expect range estimates that are large compared to the hydrophone depth. As multiple animals tend to forage at different locations, they will cluster in Figs. 6 and 7 at different angles and time delays allowing the separations of different individuals.

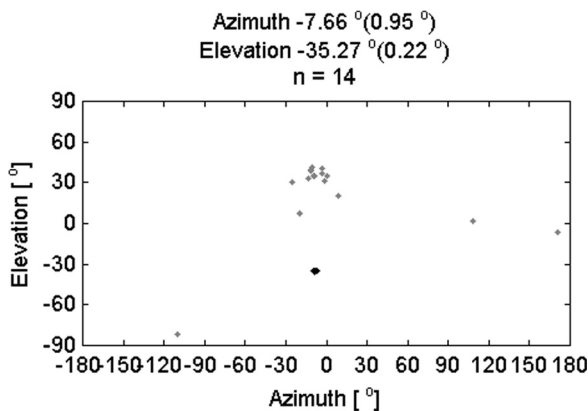


FIG. 6. Elevation-Azimuth plot of angle of arrivals. In dark are the 14 detections that can be considered to result from the animal of interest.

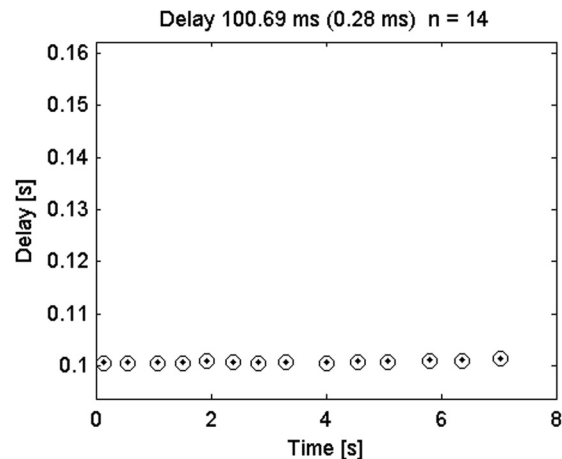


FIG. 7. Inter detection delays. Marked by circles are 14 detections that qualify for surface reflection clustering around 100.69 ms. The delay axis is limited to allowed delay values as given by Eq. (8).

These 14 pairs of elevation angles and surface reflection delays were then used together with the array depth to estimate the ranges of the individual clicks. Figure 8 shows the result of the range estimations. Both methods, geometric and ray-trace ranging, were carried out. One may note that both methods provide comparable results where the ray-tracing based range estimate (black dots in Fig. 8) resulted in somewhat shallower depth and shorter distance estimates. To generate the geometric ranging result in Fig. 8, an effective sound speed of 1516.8 m/s was used, which corresponds to the mean sound speed above the hydrophone. The geometric method overestimates the depth and range of the whale by about 20% and to obtain comparable depth and distance estimates, the effective sound speed must be increased by 0.7% to 1527.4 m/s.

Figure 8 may also be interpreted to indicate that even at distances of about 1500 m (slant ranges of about 2 km) ray bending may already become significant. This is supported by the observation from Fig. 4 that for extreme ranges, that is, for ranges where the expected range is much larger than the hydrophone depth, the direct and surface reflected rays cross with a small angle, that is, they run over a longer distance nearly parallel. Any ray bending will influence the direct path more than the steeper surface reflected path, shortening significantly the distance where both rays cross.

The relative scatter in depth and distance estimation is for both cases around 7% suggesting that observed variation will be proportional to the distance between whale and hydrophones, or that the relative scatter of both methods is nearly equal.

V. SENSITIVITY ANALYSIS

The accuracy of the localization method can be estimated with the total error differential of the distance and depth functions (e.g., [Aubauer et al., 2000](#)), which is the sum of the partial derivatives of all variables multiplied by the errors of the individual variables ([Bronstein and Semendjajew, 1983](#)).

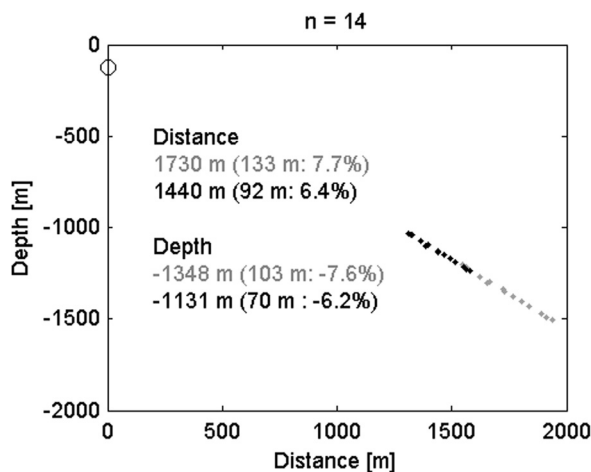


FIG. 8. Ranging of the 14 Z_c clicks for which surface reflections could be obtained. The geometric ranging (in gray) was plotted for an effective sound speed of 1516.8 m/s. The ray-tracing result is shown in black.

$$\Delta f = \left| \frac{\partial f}{\partial \tau_S} \right| \cdot |\Delta \tau_S| + \left| \frac{\partial f}{\partial \vartheta_0} \right| \cdot |\Delta \vartheta_0| + \left| \frac{\partial f}{\partial h} \right| \cdot |\Delta h|, \quad (21)$$

where f is the quantity of interest (distance X or depth z), c is the sound speed, h is the hydrophone depth, ϑ_0 is the arrival angle of the direct path, and τ_S is the time delay of the surface reflection.

Differentiating the distance and time-delay functions that are visualized in Fig. 5 with respect to the parameters τ_S , ϑ_0 , and h , one obtains the sensitivity of the range and depth estimation as function of errors in time-delay estimation, direct ray arrival angle and hydrophone depth.

Assuming the same arrival angle, time delay and hydrophone depth as used in Fig. 5, one obtains the following sensitivities: Sensitivity of depth estimation with respect to surface reflection delay error, -195.8 m/ms; with respect to angle estimation error, -438 m/ $^\circ$; or with respect to hydrophone depth error, -164.5 m/m. Obviously, these values are for the scenario of Fig. 8 and different datasets may result in different values.

From Figs. 6 and 7 one notes an elevation error of 0.22° and a time delay error of 0.28 ms; while one may deduce from Fig. 9 an error in depth estimation of 0.005 m (0.005 dBar). Combining the measurement errors Eq. (21) results to a total error of 152 m; this may be considered a reasonable upper bound of the observed error in depth estimation (70 m in Fig. 8). The contribution from the different parameters are 36% for the time delay estimation, 63% from the arrival angle estimation, and $<1\%$ from the depth estimation. These values indicate that the estimation error of the array depth alone does not contribute very much to the total error in the estimation of the whale depth.

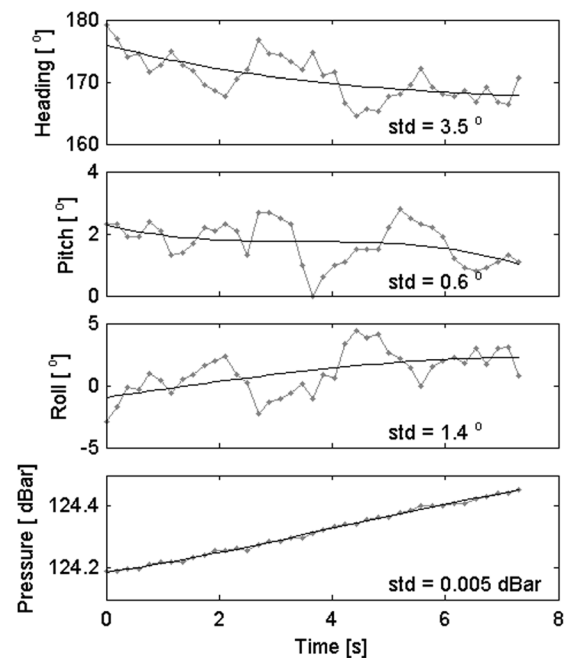


FIG. 9. Non acoustic data: heading, pitch and roll of array, measured in degrees, and water pressure, measured in dBar. In gray are the measurements and in black are the cubic interpolations. The standard deviation values are based on the difference between measured and approximated values.

Figure 8 shows that for the given scenario, all the scatter is along the direct sound path, indicating that the arrival angle estimation of the direct sound is too precise to explain the scatter in Fig. 8 leaving errors in surface delay estimation as the most likely cause of the observed scatter in Fig. 8.

This conclusion is supported by Fig. 6 where one may note that while the estimation quality of the arrival angles of the direct path seem satisfactory, the estimated arrival angles of the corresponding surface reflections scatter significantly. This is an indication that the exact arrival times of surface reflections are more difficult to obtain than the arrival times of the direct sound. This is underpinned by the observation from Fig. 2 that surface reflections are much longer than the signals of the direct arrival and have different amplitude patterns, which is equivalent to the statement that the surface reflections of this example do not only not correlate very well with the signal of the direct path, but also do not correlate among each other. This is what one expects in situations of somewhat elevated sea states where the surface roughness introduces multiple reflection points that vary randomly in depth and location resulting in statistical variations of surface reflected travel times and impeding precise estimation of the surface reflection time delay.

The presented sensitivity analysis addresses only the variability in the data, because the lack of knowledge about the real whale hydrophone geometry inhibits an assessment of the absolute error. This analysis assumes also that the observed variation in location of Fig. 8 is not due to changes in relative geometry, which can be excluded according to the following argument. As the maximal relative speed between ship and animal in this example should be less than 4 m/s (2.5 m/s ship speed and, say 1.5 m/s animal speed) the maximal closing or opening range over a period of 7 s would be ~ 30 m, which is much less than the 335 m scatter shown in Fig. 8.

While the time delays were estimated using only acoustic data, arrival angles, although originating also from acoustic data, have to be corrected with measurements of the array orientation, and errors in these measurements have a potential negative impact on the ranging performance.

Figure 9 shows the non-acoustic data for the 7 s during which the detections in Fig. 8 were made and that were used to correct the acoustically obtained signal orientation angles. The array depth was estimated from the measured water pressure and any error in this transformation would result in a common bias and not in the observed scatter. As the measured non-acoustic data turned out to be very noisy, they were approximated by cubic polygons. Figure 9 shows both the measurements and the interpolated values. The cubic approximation was chosen as it resulted in the lowest standard deviation for the estimation of the direct arrival angle (Fig. 6).

VI. SUMMARY

The present work describes the use of a towed volumetric array to estimate the range and depth of echolocating Cuvier's beaked whales. These animals are known to echolocate at depth with short ultra-sonic sounds and consequently

are relatively easily identified, mainly by the negative elevation angles of their direct sound arrivals, especially if the hydrophone array is placed at an appropriate depth. CMRE has developed the CPAM, a volumetric array of 6 hydrophones that can be towed at a depth of over 100 m, making it suitable to detect, classify, and localize Cuvier's beaked whales. The ranging method presented here consists of three-dimensional direction finding and two types of range estimation, one based on simple geometry, the other one on ray-tracing. For short distances, as is the case for beaked whale detections, both methods provide similar results, but the geometric ranging method requires the estimation of an effective sound speed, which normally is not available and may not easily be obtained in oceans with variable sound speed profiles. While the implementation of both methods is straightforward, the simplicity of the ray-tracing method suggests this method as an efficient way to incorporate ray bending. Also, the geometric ranging seems always to overestimate range and depth of vocalizing whales, as it ignores ray bending.

The presented ray-tracing method has some similarity with the method presented by Thode (2004), who used ray-tracing to track sperm whales. Both methods use ray-tracing to localize acoustic pulses, but the methods differ in the details of their implementation. Thode (2004) computed the travel times, elevation angles, and surface delay values produced by a set of sound sources placed along a grid of horizontal distances and depths. He carried out a two-dimensional grid search over range and depth for the three quantities of interest: Horizontal distance, elevation angle, and surface reflection time delay. Thode (2004) did not present the mathematical formulas he used for ray tracing, but one could assume them to be identical or similar to the one presented here. The problem Thode (2004) was faced with regarded the variable geometry of the arrays he was using. The use a compact volumetric array for direction finding simplifies the ranging method significantly and allows the estimate of range and depth with three simple one-dimensional interpolations, as arrival angles are estimated independently from the ranging method.

As to be expected, the quality of ranging methods depends on the quality of the input parameters: arrival angle, surface-reflection delay and hydrophone depth, especially for distances that exceed significantly the base-line aperture of twice the hydrophone depth. Both, the geometric ranging and the ray-tracing method suffer in similar ways from errors in these input parameters, whereby ray-tracing asks also for good knowledge about the sound speed profile. Reducing errors that are due to inadequate array-orientation estimates could help to improve the maximal useful ranging distance. Increasing the hydrophone depth could help to reduce the influence of the arrival angle estimates on the range estimate. However, this option has its limitation as with increasing hydrophone depth, the surface reflections tend to become weaker and more difficult to identify. Nevertheless, the quality of the acoustic and non-acoustic measurements of CMRE's CPAM was sufficient to result in a relative location error of less than 10%, which seems acceptable for most applications, especially when the locations are subsequently

used in tracking algorithms. Further improvement would be possible if the uncertainty in the surface reflection travel time were reduced, maybe by considering the fact that surface reflected and direct sound path should arrive from the same azimuthal angle.

ACKNOWLEDGMENTS

The presented work is part of the Active Sonar Risk Mitigation program of the NATO Science and Technology Organisation Centre for Maritime Research and Experimentation (CMRE). The CPAM has been build by CMRE's Electronic Technology Department with major contributions from Piero Guerrini, Vittorio Grandi, Luigi Troiano, Alberto Dassati, Rodney Dymond and Stefano Biagini. The author is especially grateful to Rob Been, Ryan Goldhahn and Reginald Hollett for commenting and improving the manuscript. The author would finally like to thank the principle investigators and the participants of the Sirena11 sea trials and the master and crew of NATO's Research Vessel Alliance.

- Au, W. W. L., Ford, J. K. B., Horne, J. K., and Allman, K. A. N. (2004). "Echolocation signals of free-ranging killer whales (*Orcinus orca*) and modeling of foraging for chinook salmon (*Oncorhynchus tshawytscha*)," *J. Acoust. Soc. Am.* **115**, 901–909.
- Aubauer, R., Lammers, M. O., and Au, W. W. L. (2000). "One-hydrophone method of estimating distance and depth of phonating dolphins in shallow water," *J. Acoust. Soc. Am.* **107**, 2744–2749.
- Barlow, J. (1999). "Trackline detection probability for long-diving whales," in *Marine Mammal Survey and Assessment Methods*, edited by G. W. Garner, S. C. Amstrup, J. L. Laake, B. F. J. Manly, L. L. McDonald, and D. G. Robertson (A.A. Balkema, Rotterdam, The Netherlands), pp. 209–224.
- Barlow, J., and Gisiner, R. (2006). "Mitigating, monitoring and assessing the effects of anthropogenic sound on beaked whales," *J. Cetacean Res. Manage.* **7**, 239–249.
- Bronstein, I. N., and Semendjajew, K. A. (1983). *Taschenbuch der Mathematik* (Verlag Harry Deutsch, Frankfurt), p. 152.
- Buckland, S. T., Anderson, D. R., Burnham, K. P., and Laake, J. L. (2001). *Introduction to Distance Sampling: Estimation Abundance of Biological Populations* (Oxford University Press, Oxford, UK), pp. 432.
- Clark, C. W. (1980). "A real-time direction finding device for determining the bearing to the underwater sounds of Southern Right Whales, *Eubalaena australis*," *J. Acoust. Soc. Am.* **68**, 508–511.
- Cox, T. M., Ragen, T. J., Read, A. J., Vos, E., Baird, R. W., Balcomb, K., Barlow, J., Caldwell, J., Cranford, T., Crum, L., D'Amico, A., D'Spain, G., Fernández, A., Finneran, J., Gentry, R., Gerth, W., Gulland, F., Hildebrand, J., Houser, D., Hullar, T., Jepson, P. D., Ketten, D., MacLeod, C. D., Miller, P., Moore, S., Mountain, D. C., Palka, D., Ponganis, P., Rommel, S., Rowles, T., Taylor, T., Tyack, P., Wartzok, D., Gisiner, R., Mead, J., and Benner, L. (2006). "Understanding the impacts of anthropogenic sound on beaked whales," *J. Cetacean Res. Manage.* **7**, 177–187.
- Frantzis, A. (1998). "Does acoustic testing strand whales?" *Nature* **392**, 29.
- Hirotsu, R., Yanagisawa, M., Ura, T., Akata, M., Sugimatsu, H., Kojima, J., and Bahl, R. (2010). "Localization of sperm whales in a group using clicks received at two separated short baseline arrays," *J. Acoust. Soc. Am.* **127**, 133–147.
- Jensen, F. B., Kuperman, W. A., Porter, M. B., and Schmidt, H. (2011). *Computational Ocean Acoustics*, 2nd ed. (Springer, New York), pp. 794.
- Nosal, E.-M., and Frazer, L. N. (2006). "Track of a sperm whale from delays between direct and surface-reflected clicks," *Appl. Acoust.* **67**, 1187–1201.
- Page, S. E. (1954). "Continuous inspection schemes," *Biometrika* **41**, pp. 100–115.
- Rasmussen, M. H., Lee, L. A., and Au, W. W. L. (2002). "Source levels of clicks from free-ranging white-beaked dolphins (*Lagenorhynchus albirostris* Gray 1846) recorded in Icelandic waters," *J. Acoust. Soc. Am.* **111**, 1122–1125.
- Simmonds, M. P., and Lopez-Jurado, L. F. (1991). "Whales and the military," *Nature* **337**, 448.
- Spiesberger, J. L., and Fristrup, K. M. (1990). "Passive location of calling animals and sensing of their acoustic environment using acoustic tomography," *Am. Nat.* **135**, 107–153.
- Thode, A. (2004). "Three-dimensional passive acoustic tracking of sperm whales (*Physeter macrocephalus*) in ray-refracting environments," *J. Acoust. Soc. Am.* **118**, 3575–3584.
- Tiemann, C. O., Thode, A. M., Straley, J., O'Connell, V., and Folkert, K. (2006). "Three-dimensional localization of sperm whales using a single hydrophone," *J. Acoust. Soc. Am.* **120**, 2355–2365.
- Tyack, P. L., Johnson, M., Soto, N. A., Sturlese, A., and Madsen, P. T. (2006). "Extreme diving of beaked whales," *J. Exp. Biol.* **209**, 4238–4253.
- Tyack, P. L., Zimmer, W. M. X., Moretti, D., Southall, B. L., Claridge, D. E., Durban, J. W., Clark, C. W., D'Amico, A., DiMarzio, N., Jarvis, S., McCarthy, E., Morrissey, R., Ward, J., and Boyd, I. L. (2011). "Beaked whales respond to simulated and actual navy sonar," *PLoS ONE* **6**(3), e17009, 15 p.
- Wahlberg, M., Möhl, B., and Madsen, P. T. (2001). "Estimating source position accuracy of a large-aperture hydrophone array for bioacoustics," *J. Acoust. Soc. Am.* **109**, 397–406.
- Ward, J., Morrissey, R., Moretti, D., DiMarzio, N., Jarvis, S., Johnson, M., Tyack, P., and White, C. (2008). "Passive acoustic detection and localization of *Mesoplodon densirostris* (Blainville's beaked whale) vocalizations using distributed bottom-mounted hydrophones in conjunction with a digital tag recording," *Can. Acoust.* **36**, 60–66.
- Watkins, W. A., and Schevill, W. E. (1977). "Sperm whale codas," *J. Acoust. Soc. Am.* **62**, 1485–1490.
- Wiggins, S. M., McDonald, M. A., and Hildebrand, J. A. (2012). "Beaked whale and dolphin tracking using a multichannel autonomous acoustic recorder," *J. Acoust. Soc. Am.* **131**, 156–163.
- Zimmer, W. M. X. (2011). *Passive Acoustic Monitoring of Cetaceans* (Cambridge University Press, Cambridge, UK), pp. 356.
- Zimmer, W. M. X., Harwood, J., Tyack, P. L., Johnson, M. P., Madsen, P. T. (2008). "Passive acoustic detection of deep diving beaked whales," *J. Acoust. Soc. Am.* **124**, 2823–2832.
- Zimmer, W. M. X., Johnson, M. P., D'Amico, A., and Tyack, P. L. (2003). "Combining data from a multisensor tag and passive sonar to determine the diving behavior of a sperm whale (*Physeter macrocephalus*)," *IEEE J. Ocean. Eng.* **28**, 13–28.
- Zimmer, W. M. X., Johnson, M. P., Madsen, P. T., and Tyack, P. L. (2005). "Echolocation clicks of free-ranging Cuvier's beaked whales (*Ziphius cavirostris*)," *J. Acoust. Soc. Am.* **117**, 3919–3927.

Document Data Sheet

| | | |
|--|--------------------------------------|--|
| <i>Security Classification</i> | | <i>Project No.</i> |
| <i>Document Serial No.</i> CMRE-PR-2014-005 | <i>Date of Issue</i> January 2014 | <i>Total Pages</i> 9 pp. |
| <i>Author(s)</i> Zimmer, W.M.X. | | |
| <i>Title</i> Range estimation of cetaceans with compact volumetric arrays | | |
| <i>Abstract</i> <p>Passive acoustic monitoring is the method of choice to detect whales and dolphins that are acoustically active and to monitor their underwater behaviour. The NATO Science and Technology Organization Centre for Maritime Research and Experimentation has recently implemented a compact passive acoustic monitor (CPAM), consisting of three arrays of two hydrophones each that are combined in a fixed three-dimensional arrangement and that may be towed at depths of more than 100m. With its volumetric configuration, the CPAM is capable of estimating the three-dimensional direction vector of arriving sounds and under certain conditions on relative geometry between the whale and hydrophone array, the CPAM may also estimate the range to echolocating animals. Basic ranging methods assume constant sound speed and apply straightforward geometry to obtain depth and distance to the sound source. Alternatively, ray-tracing based methods may be employed to integrate the information provided by real sound speed profiles. Both ranging methods combine measurements of sound arrival angles and surface reflection delays and are easily implemented in real-time applications, whereby one could promote the ray-tracing approach as the preferred method because it may integrate real sound speed profiles.</p> | | |
| <i>Keywords</i> | | |
| <i>Issuing Organization</i> Science and Technology Organization Centre for Maritime Research and Experimentation Viale San Bartolomeo 400, 19126 La Spezia, Italy [From N. America: STO CMRE Unit 31318, Box 19, APO AE 09613-1318] | | Tel: +39 0187 527 361 Fax: +39 0187 527 700 E-mail: library@cmre.nato.int |